

Communication

Carbon Dots Doped with Dysprosium: A Bimodal Nanoprobe for MRI and Fluorescence Imaging

Timur Sh. Atabaev ^{1,*}, Zhonglie Piao ² and Anara Molkenova ¹

¹ Department of Chemistry, School of Science and Technology, Nazarbayev University, Astana 010000, Kazakhstan; anara.molkenova@nu.edu.kz

² Wellman Center for Photomedicine, Harvard Medical School and Massachusetts General Hospital, Boston, MA 02114, USA; zpiao@mgh.harvard.edu

* Correspondence: timur.atabaev@nu.edu.kz or timuratabaev@yahoo.com; Tel.: +7-7172-70-4699

Received: 13 April 2018; Accepted: 14 May 2018; Published: 18 May 2018



Abstract: In recent years, functional nanoprobcs with multiple imaging modalities have become an emerging field of biomedical research. In this preliminary study, we utilized a facile hydrothermal method for the preparation of magneto-fluorescent bimodal carbon dots doped with dysprosium (Dy-CDs). The prepared Dy-CDs have shown a good colloidal stability in a water solution and strong blue–green fluorescence, with a maximum at 452 nm. In addition, the excellent transverse relaxivity of the prepared Dy-CDs ($r_2 = 7.42 \pm 0.07 \text{ mM}^{-1}\text{s}^{-1}$) makes them also suitable for T_2 -weighted magnetic resonance imaging (MRI). Thus, synthesized Dy-CDs could be potentially utilized for both MRI and fluorescence imaging of living cells.

Keywords: carbon dots; dysprosium; bimodal nanoprobcs; fluorescence; magnetic resonance imaging MRI

1. Introduction

The development of new nanoscale contrast agents is a promising areas of research in the field of nanomedicine. In particular, these multifunctional nanoprobcs can be more accurate than their molecular counterparts, because of the greatly improved image contrast. To date, various nanostructures, such as Fe_3O_4 [1,2], MnO [3] and various lanthanide oxides [4–7], have been successfully tested as new bimodal nanoprobcs for magnetic resonance (MR) and fluorescence imaging of living cells. On the other hand, the toxicity concerns of these inorganic nanoprobcs limit their wide usage in medical applications. To solve the toxicity issue, an appropriate surface coating should be employed with an organic layer [8], or with some inert materials, such as carbon [9] and silica [10]. However, surface modifications may affect the relaxivity properties of paramagnetic nanoprobcs and, as a result, reduce the image contrast [10]. Therefore, one can use a different strategy where the paramagnetic ions are introduced into a matrix of some biocompatible material. Paramagnetic Gd^{3+} has been incorporated into biocompatible materials such as hydroxyapatite [11], zirconia [12], and carbon [13,14]. Correspondingly, the region of interest on MRI imaging can be brighter (positive agent) because of the longitudinal relaxation that is caused by the presence of gadolinium ions. On the other hand, the negative contrast agents are more effective for bone marrow, liver, and spleen contrast enhancement [2,15]. Negative contrast nanoprobcs can be prepared using a biocompatible material that has been doped with dysprosium or holmium ions [4,16]. These nanoprobcs can generate strong MR signals thanks to the high magnetic moments of the Dy^{3+} and Ho^{3+} ions and the larger density of the magnetic ions per surface area. In this study, to the best of our knowledge, we present the first report on the synthesis and analysis of carbon dots doped with

dysprosium (Dy-CDs) ions. Thus, the main aim of this study is to demonstrate the applicability of the magneto-fluorescent Dy-CDs for simultaneous MR and optical imaging of living cells.

2. Experimental

2.1. Synthesis Process

Analytical grade dextrose $C_6H_{12}O_6$ ($\geq 99.5\%$) and dysprosium (III) chloride hexahydrate $DyCl_3 \times 6H_2O$ (99.9%) were purchased from Sigma-Aldrich (St. Louis, MO, USA) and were used as they were received. The carbon nanodots were prepared according to the reported protocols with some modification [17,18]. The solution was prepared by dissolving 2 g of dextrose in 30 mL of deionized (DI) water and was mixed with 0.1 mM of $DyCl_3 \times 6H_2O$ under continuous stirring. Next, the prepared mixtures were sealed and heated at 190 °C for 2 h. The obtained light-yellow solutions were centrifuged at 12,000 rpm for 30 min. To eliminate the unreacted products, the collected Dy-CDs were purified by dialysis in DI water for 12 h. The recollected Dy-CDs were dispersed in DI water for measurements.

2.2. Characterization

The transmission electron microscopy (TEM, JEM-2100, JEOL Ltd., Tokyo, Japan) was utilized to study the morphology of the Dy-CDs. The dynamic light scattering (DLS) size measurements were performed using a Nano ZS Zetasizer (Malvern Instruments Ltd., Malvern, UK). The photoluminescence (PL) excitation and emission spectra of the Dy-CDs were measured using a fluorescence spectrophotometer (Hitachi F-7000, Hitachi Ltd., Tokyo, Japan). The T_2 -weighted images were obtained using a 1.5 T small animal MRI scanner (Siemens Healthinners, Erlangen, Germany). The measurement parameters that were used were as follows: repetition time/echo time (TR/TE) = 2009 ms/9 ms, field of view (FOV) = 160 mm \times 160 mm, slice thickness = 5 mm, matrix = 256 \times 256, and number of excitations (NEX) = 1. All of the measurements were performed at a room temperature of 22 ± 1 °C.

3. Results and Discussion

The dissolved Dy^{3+} ions could be embedded in the carbon nanopores to form the paramagnetic Dy-CDs. According to our preliminary results, the size of these nanopores could be varied by changing the reaction time, reaction temperature, and dextrose concentration. The reaction time and concentration of the precursors were optimized in this study for the preparation of the fluorescent Dy-CDs with a high transverse relaxivity value. Figure 1 shows the size-distribution and a typical TEM image (inset) of synthesized Dy-CDs. One can see that the prepared Dy-CDs exhibited a nearly spherical shape, with the mean sizes in the range of 12–17 nm. In addition, it should be noted that the prepared Dy-CDs were highly dispersible in an aqueous solution and maintain colloidal stability for several months.

The optical properties of the prepared Dy-CDs solution were analyzed using a PL spectroscopy. Figure 2 shows the typical PL excitation and emission spectra of the Dy-CDs solution. One can see that the aqueous solution of the Dy-CDs appeared to be light-brown colored and transparent (Figure 2 inset). The prepared Dy-CDs solution exhibited an excitation-dependent emission, which was a characteristic feature for all of the carbon dots (not shown here). The excitation peak of the Dy-CDs solution reached the maximum value at ~ 363 nm. Upon a direct 363 nm excitation, the Dy-CDs solution showed the broad blue–green emission peak (Figure 2 inset) with a maximum at 452 nm. It should be mentioned that the excitation and emission peaks of the Dy-CDs solutions were red-shifted compared to the reported studies [13,14]. This red-shift was most likely as a result of the Dy and Cl doping during the synthesis process. The quantum yield (QY) of the prepared Dy-CDs solutions were measured using a quinine bisulfate solution, as the standard was 6.7%. Thus, the prepared Dy-CDs could be utilized for the fluorescence imaging of living cells [13,14].

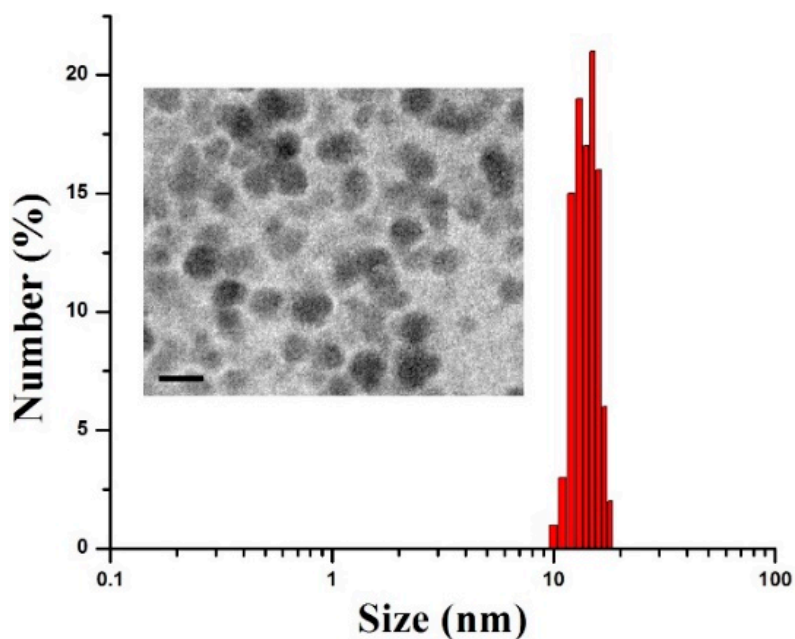


Figure 1. Size-distribution and transmission electron microscopy (TEM) image (scale bar = 20 nm) of prepared carbon dots doped with dysprosium (Dy-CDs).

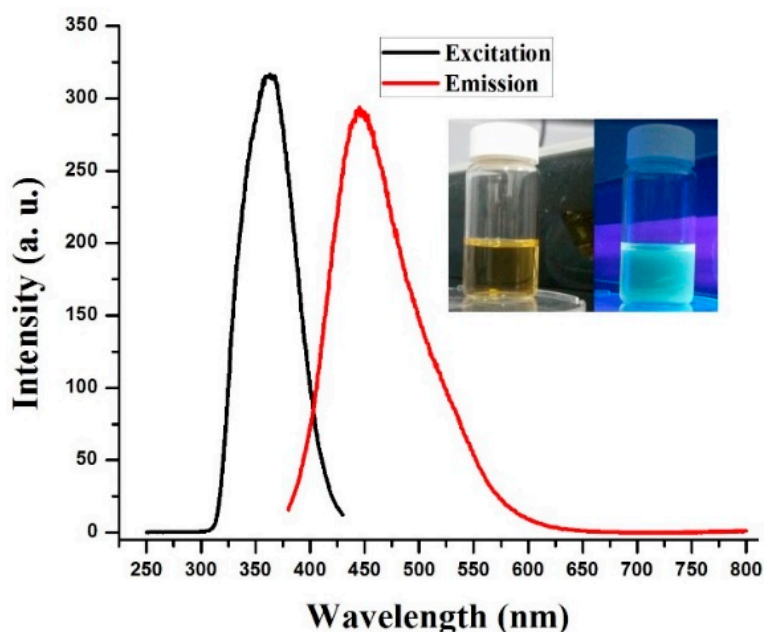


Figure 2. Photoluminescence (PL) excitation and emission spectra of the prepared Dy-CDs. Inset is a digital photo of the Dy-CDs aqueous solution, taken under daylight (left) and 365 nm UV light (right).

A small animal MRI scanner was used further in order to confirm the ability of the Dy-CDs that were to be used as contrast agents. It should be noted that the transverse relaxation was not observed in the undoped carbon dots. Figure 3 shows the $1/T_2$ curve that was measured as a function of the total Dy^{3+} concentration. The transverse relaxivity rate (r_2) was estimated from a linear fit of $1/T_2$ vs. the Dy^{3+} concentration. According to the linear fitting, the r_2 was calculated to be $7.42 \pm 0.07 \text{ mM}^{-1}\text{s}^{-1}$. The obvious darkening of the imaging site (Figure 3 inset) confirmed that the Dy^{3+} ions were successfully introduced into the carbon dots and that the Dy-CDs could be used as a

promising negative contrast agent. The Dy^{3+} and Ho^{3+} based contrast agents were especially suitable for high magnetic fields, because the r_2 value would increase with the increasing the magnetic field [16]. On the other hand, it was necessary to check how the variations of the Dy^{3+} doping concentrations affected the transverse relaxivity rate of the Dy-CDs. In addition, the toxicity of the Dy-CDs should have also been tested using several cell lines, despite the fact that the Gd-doped CDs exhibited a low toxicity [13,14]. We have planned to address the above-mentioned issues in our next full study.

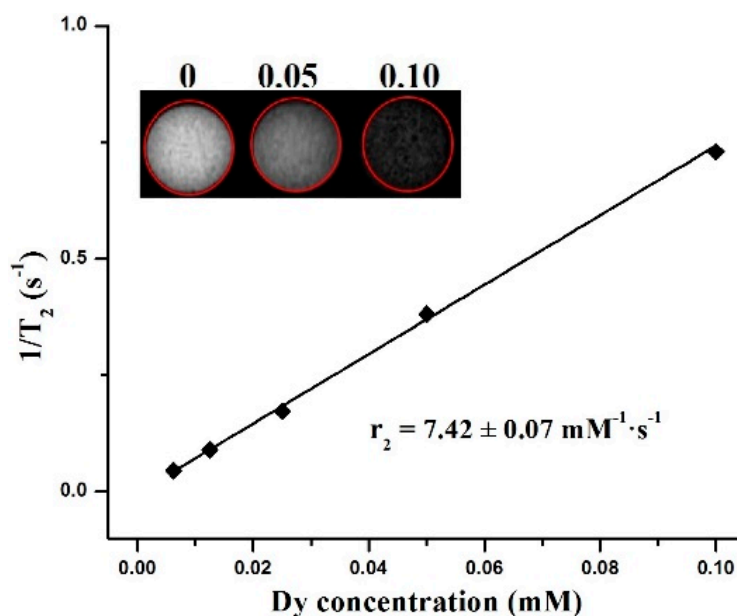


Figure 3. Transverse relaxation rate ($1/T_2$) vs. Dy^{3+} concentration (mM). Inset is the transverse relaxation images of Dy-CDs solution at different concentrations.

4. Conclusions

In summary, the bimodal Dy-doped CDs contrast nanoprobe were prepared using a facile hydrothermal synthesis method. The TEM and DLS measurements showed that the average size of the prepared Dy-CDs was about 12–17 nm. According to the PL study, the prepared Dy-CDs emitted a blue–green emission with a maximum at 452 nm. The MRI measurements of the Dy-CDs revealed that the transverse relaxivity rate (r_2) value of the sample was $7.42 \pm 0.07 \text{ mM}^{-1} \text{ s}^{-1}$. We strongly believe that the prepared bifunctional Dy-CDs can be of great interest for MRI and fluorescence imaging of living cells.

Author Contributions: T.S.A. designed the experiments, T.S.A. and A.M. performed the synthesis and characterization of the samples, T.S.A. and Z.P. analyzed the data, and T.S.A. wrote the manuscript.

Acknowledgments: This work was supported by the Social Policy Grant that was provided by Nazarbayev University to conduct the preliminary research.

Conflicts of Interest: The authors declare no conflict of interest.

References

- Gu, J.; Zhang, W.; Yang, X. Preparation of a superparamagnetic MRI contrast agent with a tumor targeting function. *Mater. Lett.* **2013**, *94*, 8–10. [[CrossRef](#)]
- Atabaev, T.S. PEG-coated superparamagnetic dysprosium-doped Fe_3O_4 nanoparticles for potential MRI imaging. *BioNanoScience* **2018**, *8*, 299–303. [[CrossRef](#)]
- Chen, N.; Shao, C.; Qu, Y.; Li, S.; Gu, W.; Zheng, T.; Ye, L.; Yu, C. Folic acid-conjugated MnO nanoparticles as a T_1 contrast agent for Magnetic Resonance imaging of tiny brain gliomas. *ACS Appl. Mater. Interfaces* **2014**, *6*, 19850–19857. [[CrossRef](#)] [[PubMed](#)]

4. Norek, M.; Kampert, E.; Zeitler, U.; Peters, J.A. Tuning of the size of Dy₂O₃ nanoparticles for optimal performance as an MRI contrast agent. *J. Am. Chem. Soc.* **2008**, *130*, 5335–5340. [[CrossRef](#)] [[PubMed](#)]
5. Atabaev, T.S.; Lee, J.H.; Han, D.-W.; Kim, H.-K.; Hwang, Y.-H. Ultrafine PEG-capped gadolinia nanoparticles: Cytotoxicity and potential biomedical applications for MRI and luminescent imaging. *RSC Adv.* **2014**, *4*, 34343–34349. [[CrossRef](#)]
6. Atabaev, T.; Lee, J.; Shin, Y.; Han, D.-W.; Choo, K.; Jeon, U.; Hwang, J.; Yeom, J.; Kim, H.-K.; Hwang, Y.-H. Eu, Gd-Codoped Yttria Nanoprobes for Optical and T₁-Weighted Magnetic Resonance Imaging. *Nanomaterials* **2017**, *7*, 35. [[CrossRef](#)] [[PubMed](#)]
7. Xu, W.; Kattel, K.; Park, J.Y.; Chang, Y.; Kim, T.J.; Lee, G.H. Paramagnetic nanoparticle T₁ and T₂ MRI contrast agents. *Phys. Chem. Chem. Phys.* **2012**, *14*, 12687. [[CrossRef](#)] [[PubMed](#)]
8. Yu, M.; Huang, S.; Yu, K.J.; Clyne, A.M. Dextran and polymer polyethylene glycol (PEG) coating reduce both 5 and 30 nm iron oxide nanoparticle cytotoxicity in 2D and 3D cell culture. *Int. J. Mol. Sci.* **2012**, *13*, 5554–5570. [[CrossRef](#)] [[PubMed](#)]
9. Atabaev, T.S.; Lee, J.H.; Han, D.-W.; Kim, H.-K.; Hwang, Y.-H. Fabrication of carbon coated gadolinia particles for dual-mode magnetic resonance and fluorescence imaging. *J. Adv. Ceram.* **2015**, *4*, 118–122. [[CrossRef](#)]
10. Atabaev, T.S.; Lee, J.H.; Han, D.W.; Choo, K.S.; Jeon, U.B.; Hwang, J.Y.; Yeom, J.A.; Kang, C.; Kim, H.K.; Hwang, Y.H. Multicolor nanoprobes based on silica-coated gadolinium oxide nanoparticles with highly reduced toxicity. *RSC Adv.* **2016**, *6*, 19758–19762. [[CrossRef](#)]
11. Tesch, A.; Wenisch, C.; Herrmann, K.H.; Reichenbach, J.R.; Warncke, P.; Fischer, D.; Müller, F.A. Luminomagnetic Eu³⁺- and Dy³⁺-doped hydroxyapatite for multimodal imaging. *Mater. Sci. Eng. C* **2017**, *81*, 422–431. [[CrossRef](#)] [[PubMed](#)]
12. Atabaev, T.S. Paramagnetic Gd-doped zirconia nanoparticles for potential T₁-weighted MRI imaging. *Nano Life* **2017**, *7*, 1750007. [[CrossRef](#)]
13. Ren, X.Y.; Yuan, X.X.; Wang, Y.P.; Liu, C.L.; Qin, Y.; Guo, L.P.; Liu, L.H. Facile preparation of Gd³⁺ doped carbon quantum dots: Photoluminescence materials with magnetic resonance response as magnetic resonance/fluorescence bimodal probes. *Opt. Mater.* **2016**, *57*, 56–62. [[CrossRef](#)]
14. Yu, C.; Xuan, T.; Chen, Y.; Zhao, Z.; Liu, X.; Lian, G.; Li, H. Gadolinium-doped carbon dots with high quantum yield as an effective fluorescence and magnetic resonance bimodal imaging probe. *J. Alloys Compd.* **2016**, *688*, 611–619. [[CrossRef](#)]
15. Briley-Saebo, K.; Bjørnerud, A.; Grant, D.; Ahlstrom, H.; Berg, T.; Kindberg, G.M. Hepatic cellular distribution and degradation of iron oxide nanoparticles following single intravenous injection in rats: Implications for magnetic resonance imaging. *Cell Tissue Res.* **2004**, *316*, 315–323. [[CrossRef](#)] [[PubMed](#)]
16. Atabaev, T.S.; Shin, Y.C.; Song, S.-J.; Han, D.-W.; Hong, N.H. Toxicity and T₂-weighted magnetic resonance imaging potentials of holmium oxide nanoparticles. *Nanomaterials* **2017**, *7*, 216. [[CrossRef](#)] [[PubMed](#)]
17. Liang, Q.; Ma, W.; Shi, Y.; Li, Z.; Yang, X. Easy synthesis of highly fluorescent carbon quantum dots from gelatin and their luminescent properties and applications. *Carbon* **2013**, *60*, 421–428. [[CrossRef](#)]
18. Zhou, J.; Shan, X.; Ma, J.; Gu, Y.; Qian, Z.; Chen, J.; Feng, H. Facile synthesis of P-doped carbon quantum dots with highly efficient photoluminescence. *RSC Adv.* **2014**, *4*, 5465. [[CrossRef](#)]

